PHYSICAL REVIEW E **84**, 015102(R) (2011)

Role of modulus mismatch on crack propagation and toughness enhancement in bioinspired composites

Palla Murali,[1] Tanmay K. Bhandakkar,[2] Wei Li Cheah,[3] Mark H. Jhon,[1]
Huajian Gao,[2] and Rajeev Ahluwalia[1,*]

[1]*Institute of High Performance Computing, Singapore, 138632*
[2]*School of Engineering, Brown University, Providence, Rhode Island 02912, USA*
[3]*Institute of Materials Research and Engineering, Singapore, 117602*

(Received 6 January 2011; revised manuscript received 9 May 2011; published 18 July 2011; publisher error corrected 22 July 2011)

Natural materials such as nacre exhibit a high resistance to crack propagation, inspiring the development of artificial composites imitating the structure of these biological composites. We use a phase field approach to study the role played by the elastic modulus mismatch between stiff and soft layers on crack propagation in such bioinspired composites. Our simulations show that the introduction of a thin layer of a soft phase in a stiff matrix can lead to arrest of a propagating crack and can also lead to crack branching. The crack branching observed in the phase field model is analyzed using a cohesive zone approach. Further, we show that the toughness of such a composite can be substantially higher than that of its constituents.

DOI: 10.1103/PhysRevE.84.015102 PACS number(s): 46.50.+a, 87.85.jc, 46.15.−x, 62.20.mm

Natural composites of a stiff mineral phase and soft organic phase are ubiquitous in biological materials [1]. For example, bone is a composite of the mineral hydroxyapatite, and the protein collagen, which are arranged in a hierarchical manner over length scales ranging from tens of nanometers to several hundred microns [2]. Similarly, nacre, a constituent of some sea shells, is a composite of the mineral aragonite and a variety of biopolymers. A striking property of such materials is that although the components are brittle, the composite may have exceptional fracture resistance. A variety of toughening mechanisms have been observed in such materials. In bone, for example, crack deflection at weak interfaces, microcracking, bridging due to uncracked ligaments, and bridging of collagen fibrils have been suggested to contribute to the toughness [3,4]. The spatially varying elastic modulus also has been proposed to increase the toughness of these composites. For example, crack arrest and crack kinking have been observed and attributed to the different elastic moduli of different layers in teeth [5]. Further, recent theoretical studies have found that periodic variations of the modulus are enough to cause a crack to arrest at a soft layer [6–8]. The understanding of these toughening mechanisms in biocomposites has important implications for engineering materials with superior resistance to fracture.

By mimicking the layered structure of nacre, for instance, researchers have successfully enhanced the fracture toughness of artificial composites [9]. Toughening mechanisms in these bioinspired composites may be distinct from those observed in biological materials. For example, in natural biocomposites, mineral grains are nanosized, making them insensitive to flaws [8]. This is not necessarily true for bioinspired composites (and composites in general) as the length scales are usually larger. However, a feature common to both biocomposites and bioinspired composites is the extreme modulus mismatch, the disparity in the stiffness between the components. This leads us to ask the following generic question: How will the propagation of a crack in the composite be influenced by the presence of a thin, soft layer? In order to answer this question, there is a need to develop a dynamical framework that can describe the path of a crack in an inhomogeneous medium.

The phase field method has recently emerged as a powerful technique to study the dynamics of fracture and crack propagation in homogeneous brittle materials [10–12] as well as composite systems [13,14]. In the phase field approach, an order parameter that characterizes the degree of brokenness of a material is coupled to elasticity via a phenomenological Ginzburg–Landau-type energy function. This approach is well suited to study crack propagation in composite materials because no *a priori* assumption of the crack path is required. The crack path is determined by the coupling between the order parameter and the elastic stresses. Thus, the interaction of a crack with a complex, inhomogeneous microstructure can be studied in an unbiased manner.

In this paper, we apply the phase field method to study crack propagation in a simple model system that contains some basic features of bioinspired composites. A cohesive zone model is used to phenomenologically explain the crack paths predicted by the phase field model. We focus on the following issue: What factors determine the crack path in the vicinity of interfaces between stiff and soft materials? Further, we also investigate the enhancement in toughness of the composite due to the modulus mismatch between the constituents.

The present phase field model is formulated in terms of an order parameter $\phi(\vec{r})$, which describes the degree of brokenness of the solid, i.e., $\phi(\vec{r}) = 1$ corresponds to the unbroken solid and $\phi(\vec{r}) = 0$ inside the crack. The order parameter is coupled to the elastic energy via a free energy functional that can be expressed as

$$F = \int d\vec{r} \left[g(\phi)(E_{\text{elas}} - E_{\text{th}}) + \frac{K}{2}(\vec{\nabla}\phi)^2 \right]. \qquad (1)$$

The function $g(\phi) = 4\phi^3 - 3\phi^4$ is 0 inside the crack and 1 in the solid. The elastic energy density is given by $E_{\text{elas}} = \lambda(\vec{r})\varepsilon_{kk}^2/2 + \mu(\vec{r})\varepsilon_{ij}\varepsilon_{ij}$, where $\varepsilon_{ij} = 0.5(\partial u_i/\partial x_j + \partial u_j/\partial x_i)$ is the linearized strain tensor, obtained from the displacement

*Corresponding author: rajeev@ihpc.a-star.edu.sg

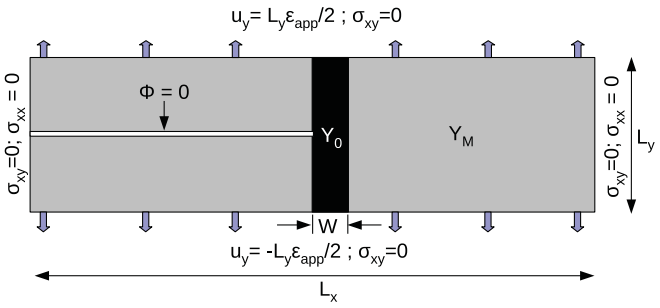

FIG. 1. (Color online) Schematic of the simulation domain indicating the loading conditions and the geometry for simulations of dynamic crack propagation. A macroscopic applied strain ε_{app} is applied to the top and bottom face.

field u_i; E_{th} represents a threshold strain energy density such that the material will fail when $E_{\text{elas}} > E_{\text{th}}$; $\lambda(\vec{r}) = Y(\vec{r})\nu/(1+\nu)(1-2\nu)$ and $\mu(\vec{r}) = Y(\vec{r})/2(1-\nu)$, where $Y(\vec{r})$ is a position dependent Young's modulus and ν is Poisson's ratio. The gradient term K is related to the surface energy γ by $K = \gamma^2/E_{\text{th}}$ [10–12]. The dynamics of crack propagation are simulated by solving coupled equations for the order parameters and the displacement fields:

$$\frac{d\phi}{dt} = -M\frac{\delta F}{\delta \phi} = -M[-K\nabla^2\phi + (E_{\text{elas}} - E_{\text{th}})\, g'(\phi)], \quad (2)$$

$$\rho\frac{d^2u_i}{dt^2} = \frac{\partial \sigma_{ij}}{\partial x_j} + \eta\nabla^2\frac{du_i}{dt}, \quad (3)$$

where M is the mobility which sets the time scale of crack propagation, ρ is the density, η is the viscosity, and $\sigma_{ij} = (\lambda\delta_{ij}\varepsilon_{kk} + 2\mu\varepsilon_{ij})g(\phi)$ are the components of the stress tensor.

The objective of the present analysis is to explore the underlying mechanisms of crack propagation in a generic, rather than a specific material system. Thus, we introduce a characteristic length scale given as $\delta = \gamma/E_{\text{th}}$ and a characteristic time scale given by $\tau = 1/ME_{\text{th}}$. We choose the following rescaled parameters in the present simulations, $K' = (K/E_{\text{th}}\delta^2) = 4$, $\rho' = (\rho/E_{\text{th}})(\delta/\tau)^2 = 1$, $\eta' = \eta/E_{\text{th}}\tau = 2$, and $\gamma' = \gamma/E_{\text{th}}\delta = \sqrt{K'}$.

Since the aim of this study is to understand the role played by modulus mismatch on crack propagation, we consider a very simple, two-dimensional model composite of two components having different elastic moduli. By analogy to nacre, we refer to the stiff component as the "mineral" and the soft component as the "organic." We study the fracture of this composite while varying the Young's modulus of the organic layer, Y_O. This has the effect of altering the modulus mismatch, Y_O/Y_M, where Y_M is the Young's modulus of the mineral component. The threshold energy density E_{th} and Poisson's ratio $\nu = 0.27$ are taken to be the same for both components.

We consider a sandwich structure consisting of a very thin, soft organic layer placed between two thicker, stiff mineral plates. One plate is precracked, with the crack terminating at the mineral-organic interface, as shown in Fig. 1. This geometry is taken to roughly reflect that of some recently fabricated bioinspired materials [9]. The dynamic fracture of this structure is analyzed by integrating Eqs. (2) and (3) using a finite difference scheme with grid spacing $\Delta x = \Delta y = \delta$ and time step $\Delta t = 0.01\tau$. The simulation domain is a rectangular grid of dimension $L_x \times L_y$ where $L_x = 900\delta$, $L_y = 300\delta$. The width of the organic layer is $W = 27\delta$. A precrack is initialized by setting $\phi = 0$ inside the crack and $\phi = 1$ outside. A macroscopic strain ε_{app} is applied to the composite by imposing $u_y = L_y\varepsilon_{\text{app}}/2$, $\sigma_{xy} = 0$ at the top face and $u_y = -L_y\varepsilon_{\text{app}}/2$, $\sigma_{xy} = 0$ at the bottom face. A traction-free boundary condition ($\sigma_{xx}, \sigma_{xy} = 0$) is applied to the left and right sides.

To simulate crack propagation, a fixed macroscopic strain ε_{app} is imposed and the evolution of the crack is monitored until the cracks either stop evolving or reach the other end. The simulations are repeated for different values of ε_{app} and Y_O/Y_M. Figure 2 depicts crack propagation in the composites with $Y_O/Y_M = 0.32$, $Y_O/Y_M = 0.10$, and $Y_O/Y_M = 0.01$. For the case of $Y_O/Y_M = 0.32$, the crack at the interface starts to move into the organic layer for strains of $\varepsilon_{\text{app}} > 0.15$. However, the crack does not proceed all the way through the composite, but instead arrests in the organic layer. Upon increasing the load, the arrested crack moves deeper into the organic but arrests again. The loading may be further increased until the crack moves out of the organic at $\varepsilon_{\text{app}} > 0.26$, causing the

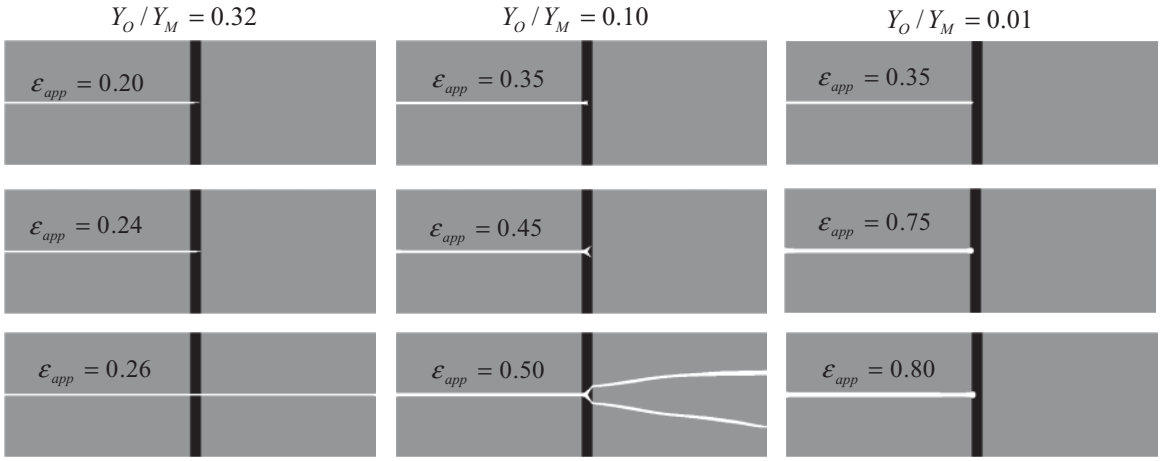

FIG. 2. Final crack patterns from the phase field simulations for different values of the macroscopic applied strain ε_{app}. The ratio Y_O/Y_M represents the Young's modulus ratio of the soft organic layer (black region) and the stiff mineral layer (grey region).

composite to fail. The path of the crack is straight and does not show any branching. Crack arrest is also observed for $Y_O/Y_M = 0.10$ but the strains required for crack initiation and crack propagation are much higher compared to $Y_O/Y_M = 0.32$. In addition, for $\varepsilon_{\text{app}} > 0.35$, we observe crack branching. This can be clearly seen in Fig. 2 by examining the crack profiles for $Y_O/Y_M = 0.10$. Increasing the strain further leads to both branches growing until they exit the organic layer and the composite fails. For the case of $Y_O/Y_M = 0.01$, the crack tip arrests in the organic layer for strains up to $\varepsilon_{\text{app}} = 0.80$. Upon further increasing ε_{app}, a second crack initiates in the mineral plate that is ahead of the organic layer. The composite fails once this crack merges with the first crack. The main observations from these simulations are that for sufficiently large values of the elastic modulus mismatch, (1) cracks can arrest in the organic layer and require increasingly higher loads for the cracks to move out of the organic layer, (2) cracks can branch at higher strains, and (3) increasing the elastic modulus mismatch increases the tendency of cracks to both arrest and branch.

Why does the crack arrest inside the organic layer? To address this question, we calculate the driving force for straight crack propagation inside the organic layer, $G = -\partial\Gamma/\partial a$. In this expression, $\Gamma = \int g(\phi)E_{\text{elas}}d\vec{r}$ is the elastic energy and a is the crack length. G is calculated by computing Γ obtained from the phase field simulations for different values of initial crack length a. The threshold energy density E_{th} is kept high enough so that the crack does not propagate, even at high strains. The critical driving force for crack propagation through a homogeneous material is $G_c = 2\gamma$. Figure 3 plots G/G_c vs a_0/W for different values of Y_O/Y_M at a fixed value of $\varepsilon_{\text{app}} = 0.25$. Here a_0 denotes the length of the crack that is inside the organic layer. For the homogeneous case, the driving force remains constant as the crack advances. For the composite, we observe that the driving force decreases as the crack propagates inside the organic layer [7]. It is observed that $G > G_c$ for all crack lengths when $Y_O/Y_M > 0.10$. For $Y_O/Y_M = 0.10$, the driving force falls below the critical driving force G_c when the crack length exceeds a critical value. This explains why cracks arrest in the middle of the organic layer as observed

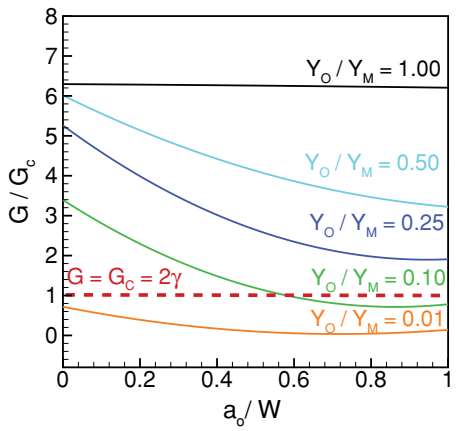

FIG. 3. (Color online) Normalized strain energy release rate G/G_C vs crack length a_0/W for composites of different Young's modulus ratios. Here a_0 is the crack length inside the organic component, and W is the width of the organic layer. $G_C = 2\gamma$ is the critical driving force for crack propagation.

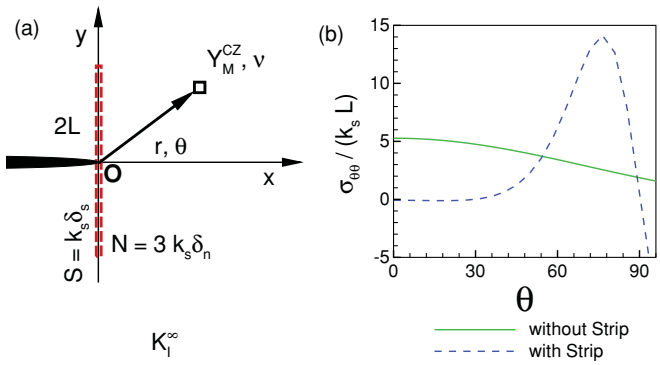

FIG. 4. (Color online) (a) Schematic for the cohesive zone model. (b) Variation of circumferential stress $\sigma_{\theta\theta}$ with angle θ with (solid line) and without (dashed line) the presence of the soft strip.

in Fig. 2. For the case with $Y_O/Y_M < 0.10$, we observe that $G < G_c$ for all crack lengths and hence the crack will not propagate at this particular strain. This analysis shows that the modulus mismatch can reduce the local driving force for crack propagation, causing cracks to arrest in the soft layer.

In addition to, or in lieu of arresting, cracks may branch as they pass through a soft layer. The branching illustrated in Fig. 2 appears to be distinct from crack branching observed in prior phase field studies [11]. Previous studies have attributed branching to a dynamic mechanism associated with high speed cracks in brittle materials [15,16], while we measure crack speeds much smaller than that required for dynamic branching. Instead, we find that the modulus mismatch leads to the crack-tip stress field bifurcating. By analogy to Yoffe's analysis of high speed cracks, this bifurcation can lead to branching [16]. The stress field bifurcation can be demonstrated with a static calculation using a cohesive zone model. As illustrated in Fig. 4(a), we consider a stationary, semi-infinite crack subjected to a remote Mode I loading under plane strain conditions in an isotropic elastic medium, with a soft strip oriented normal to the crack plane and centered at the crack tip. The soft strip is modeled as a cohesive zone of length $2L$, where the normal and shear tractions are, respectively, given as $N = 3k_s\delta_n$ and $S = k_s\delta_s$. δ_n and δ_s are the normal and slip displacements and k_s is the stiffness of the cohesive zone. The cohesive zone is described as a continuous distribution of infinitesimal dislocations [17]. Integral equations are set up for the deformation in the soft strip and solved numerically. In the calculation, the remote stress intensity factor is $K_I^\infty = 1.0k_sL^{3/2}$ and the strip is ten times softer than the surrounding medium. This sets $Y_O^{CZ}/Y_M^{CZ} = 0.10$, where the effective modulus of the soft strip is $Y_O^{CZ} = k_sL$ and the plane strain Young's modulus of the matrix is Y_O^{CZ}. Figure 4(b) shows the angular variation of the circumferential stress $\sigma_{\theta\theta}$ evaluated at a distance $r/L = 5.7 \times 10^{-3}$ away from the crack tip, with and without the presence of a soft strip. It is observed that the orientation of maximum $\sigma_{\theta\theta}$ shifts from $\theta = 0^\circ$ in the homogeneous case to $\theta \approx 75^\circ$ in the presence of a soft strip, which supports our phase field simulation results on crack branching. It is interesting to note the similarity between the results of the present cohesive zone solution and Yoffe's analysis of high speed cracks [16]. Both solutions predict a shift in orientation of the maximum circumferential stress

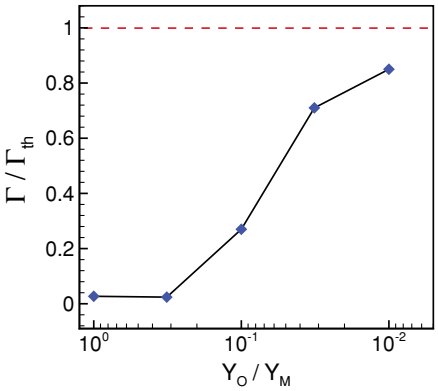

FIG. 5. (Color online) Normalized composite toughness $\Gamma/\Gamma_{\text{th}}$ vs modulus mismatch Y_O/Y_M computed from phase field simulations.

from $\theta = 0^\circ$ to $\theta \approx 75^\circ$. We believe that the bifurcation of the crack-tip stress fields may have important implications for the fracture behavior of bioinspired composites.

How does the modulus mismatch influence the toughness of the composite? Although the G_c of each component is not affected by the structure of the composite, the structural features in the composite can still affect crack propagation. For example, Figs. 2 and 3 clearly show that cracks can arrest and branch in the soft layer. We characterize the toughness Γ_f of the composite as the elastic energy Γ evaluated at the largest applied strain before fracture, $\varepsilon_{\text{app}} = \varepsilon_f$, where ε_f, is the fracture strain. Γ_f and ε_f are obtained by repeating the phase field crack propagation simulations in Fig. 2 for different values of ε_{app} for each value of Y_O/Y_M. The maximum toughness is taken as $\Gamma_{\text{th}} = E_{\text{th}}\Omega$, where Ω is the volume of the sample. When $\Gamma_f = \Gamma_{\text{th}}$, the composite can fail even in the absence of any defects (cracks). Figure 5 plots the normalized toughness $\Gamma_f/\Gamma_{\text{th}}$ for various values of Y_O/Y_M. The normalized toughness $\Gamma_f/\Gamma_{\text{th}}$ of the composite increases rapidly as the modulus mismatch Y_O/Y_M decreases, approaching the maximum value Γ_{th} as $Y_O/Y_M \to 0$. Remarkably, the toughness for the $Y_O/Y_M = 0.01$ case is approximately thirty times that of the pure mineral and ~0.9 times the maximum toughness Γ_{th}. This means that when the organic layer is very soft, the failure of a composite in the phase field model is governed by the theoretical strength of its constituents.

In summary, we have studied crack propagation in a model composite system using a phase field approach. Our simulations predict that propagating cracks can arrest inside the soft layer and show a tendency to branch as they pass through the soft layer. This branching behavior is consistent with the predictions of a cohesive zone model. Estimates of the toughness based on the phase field model show that when the modulus of the soft layer is very low, the toughness of the composite is limited by the theoretical strength of the components. Artificial composites may be designed to take advantage of our finding that very thin, soft layers can cause branching and toughness enhancement. We end this paper with the outlook that phase field fracture models can become an extremely useful tool to help design composite materials with superior mechanical properties.

ACKNOWLEDGMENTS

The authors would like to thank David Srolovitz, Justin Song, Srikanth Vedantam, Bin Chen, Ramarathinam Narasimhan, and Yongwei Zhang for useful discussions. The work of P.M. and H.G. has been supported by the A∗STAR Visiting Investigator Program "Size Effects in Small Scale Materials."

[1] M. A. Meyers *et al.*, Prog. Mater. Sci. **53**, 1 (2008); P. Fratzl and R. Weinkamer, *ibid.* **52**, 1263 (2007); H. Gao, Int. J. Fract. **138**, 101 (2006).
[2] K. J. Koester *et al.*, Biomaterials **29**, 1318 (2008).
[3] K. J. Koester *et al.*, Nat. Mater. **7**, 672 (2008).
[4] M. Sarikaya *et al.*, Mater. Res. Soc. Symp. Proc. **174**, 109 (1989).
[5] S. Bechtle *et al.*, Biomaterials **31**, 4238 (2010).
[6] K. Okumura and P. G. de Gennes, Eur. Phys. J. E: Soft Matter Biol. Phys. **4**, 121 (2001).
[7] P. Fratzl *et al.*, Adv. Mater. **19**, 2657 (2007); H. J. Gao, Int. J. Solids Struct. **27**, 1663 (1991).
[8] B. H. Ji and H. J. Gao, Mater. Sci. Eng. A **366**, 96 (2004); H. J. Gao *et al.*, Proc. Natl. Acad. Sci. USA **100**, 5597 (2004).
[9] E. Munch *et al.*, Science **322**, 1516 (2008).
[10] A. J. Pons and A. Karma, Nature **464**, 85 (2010).
[11] A. Karma and A. E. Lobkovsky, Phys. Rev. Lett. **92**, 245510 (2004).
[12] H. Henry and H. Levine, Phys. Rev. Lett. **93**, 105504 (2004).
[13] S. B. Biner and S. Y. Hu, Acta Mater. **57**, 2088 (2009).
[14] G. P. Zheng and Y. Shen, Int. J. Solids Struct. **47**, 320 (2010).
[15] M. Adda-Bedia, R. Arias, M. BenAmar, and F. Lund, Phys. Rev. Lett. **82**, 2314 (1999).
[16] E. H. Yoffe, Philos. Mag. **42**, 739 (1951).
[17] B. A. Bilby *et al.*, Proc. R. Soc. London, Ser. A **272**, 304 (1963).